

Dalton Transactions

Accepted Manuscript



This is an *Accepted Manuscript*, which has been through the Royal Society of Chemistry peer review process and has been accepted for publication.

Accepted Manuscripts are published online shortly after acceptance, before technical editing, formatting and proof reading. Using this free service, authors can make their results available to the community, in citable form, before we publish the edited article. We will replace this *Accepted Manuscript* with the edited and formatted *Advance Article* as soon as it is available.

You can find more information about *Accepted Manuscripts* in the [Information for Authors](#).

Please note that technical editing may introduce minor changes to the text and/or graphics, which may alter content. The journal's standard [Terms & Conditions](#) and the [Ethical guidelines](#) still apply. In no event shall the Royal Society of Chemistry be held responsible for any errors or omissions in this *Accepted Manuscript* or any consequences arising from the use of any information it contains.

Trivalent acid radical-centered YLi_4^+ ($Y = PO_4, AsO_4, VO_4$) cations: new polynuclear species designed to enrich the superalkali family

Jia-Yuan Liu, Di Wu, Wei-Ming Sun, Ying Li,* Zhi-Ru Li

Institute of Theoretical Chemistry, State Key Laboratory of Theoretical and Computational Chemistry, Jilin University, Changchun 130023, People's Republic of China

ABSTRACT

A new series of polynuclear superalkali cations YLi_4^+ ($Y = PO_4, AsO_4, VO_4$) has been characterized using ab initio methods. The central Y^{3-} ($PO_4^{3-}, AsO_4^{3-}, VO_4^{3-}$) acid radicals preserve their structural and electronic integrity in the first several lowest-lying isomers of YLi_4^+ . Meanwhile, the introduction of Li^+ cations can also dissociate an O^{2-} ion from the Y^{3-} groups. Besides, the AsO_4^{3-} group is discerned to be separated into AsO_2^- and O_2^{2-} fragments other than AsO_3^- and O^{2-} units. This is why the $AsO_4Li_4^+$ cation has been found to possess more diverse structures.

The vertical electron affinities (EA_{vert}) of the YLi_4^+ cations range from 2.44 to 4.67 eV, which are low enough to validate the superalkali or pseudoalkali identity of the title species. It is also noteworthy that the YLi_4^+ conformer with T_d symmetry makes for a more even distribution of the excess positive charge, and consequently exhibits the lowest EA_{vert} value of ca. 2.45 eV.

*Corresponding author.
Email address: liyingedu@jlu.edu.cn

1. Introduction

During the last few years, numerous investigations have been conducted to explore the structural and electronic properties of atomic and molecular clusters. One of the most exciting developments in cluster science is the realization that selected clusters could mimic the electronic behavior of atoms of similar valence states and hence be regarded as superatoms.^{1,2} A well-known subset of superatoms is superalkali,³⁻¹⁰ which is characterized by lower ionization potentials (IPs) than those (5.4–3.9 eV)¹¹ of alkali-metal atoms. Over the past decades, the hyperalkalized compounds ML_{k+n} (where L is an alkali metal atom, k is the maximal formal valence of the central atom M, and $n \geq 1$) which was introduced by Gutsev and Boldyrev,³ have become the major part of investigated superalkalis because they often exhibit very low IPs.

The superalkalis are of great importance in chemistry. On the one hand, they possess excellent reducibility and can be used in the synthesis of novel charge-transfer salts in which the corresponding anions are formed by the species with low electron affinity. For example, the true natures of the Li_3NO_3 and Na_3NO_3 compounds have been identified to be $(Li_3O)^+NO_2^-$ ¹² and $(Na_3O)^+NO_2^-$,¹³⁻¹⁵ respectively, where the superalkali cations Li_3O^+ and Na_3O^+ are contained. On the other hand, superalkalis are at an advantage in cases where the formation of the corresponding salts with alkali metal atoms is not promising because of steric hindrance. Castleman and co-workers have indicated that the size of the Al_{13} superhalogen is too big to fit with counterions such as the alkali metals. Thus they have proposed using the larger superalkali cationic motifs (Na_3O and K_3O) to overcome this size mismatch.¹⁶ Furthermore, superalkalis have been found to maintain their structural and electronic integrities inside various superatom compounds, such as Li_3-SH ($SH = LiF_2, BeF_3, BF_4$)¹⁷, $Al_{13}(K_3O)$ ¹⁶ and $Al_{13}(Na_3O)$,¹⁶ $B Li_6-X$ ($X = F, LiF_2, BeF_3, BF_4$),¹⁸ Na_2XY ($X = SCN, OCN, CN; Y = MgCl_3, Cl, \text{ and } NO_2$),¹⁹ BF_4-M ($M = Li, FLi_2, OLi_3, NLi_4$),²⁰ $Li_3O(BF_4)$,²¹ $Li_3O(BeF_3)$ ²¹ and $Li_3O(NO_3)$ ²¹ etc. Therefore, superalkalis may represent potential building blocks for the assembly of new materials in which strong electron donors are involved.

Based on the above-mentioned features, the superalkali clusters have attracted more and more attention in recent years and many efforts have been devoted to designing and characterizing new superalkalis. Hitherto several kind of unconventional superalkalis have been proposed. In our previous works, a series of binuclear superalkalis of the $M_2Li_{2k+1}^+$ type were theoretically predicted.^{7,8} Meanwhile, the investigations on superalkali were also extended to include the polynuclear species with acid groups as the central core. Such an attempt begins by using halogenoids X (SCN, OCN, and CN) and alkali metal atoms to construct superalkalis Li_2X and Na_2X .²² Afterwards, the familiar bivalent acid groups CO_3^{2-} , SO_3^{2-} , and SO_4^{2-} and oxygen-rich dianions O_4^{2-} and O_5^{2-} were chosen to play the role of the central core of superalkali cations YLi_3^+ .²³ Most recently, a series of polynuclear superalkali cations with the same YLi_3^+ formula (Y represents peroxides O_2 , CO_4 , C_2O_4 , and C_2O_6) have been described in detail.²⁴ These achievements demonstrate that the potential of creating new species classified as superatoms is limitless and thereby motivate us to explore more new superalkalis and further enrich the superalkali family.

In the present work, we set the trivalent acid radicals (PO_4^{3-} , AsO_4^{3-} , VO_4^{3-}) as the central core and get a novel series of polynuclear superalkali cations YLi_4^+ (Y = AsO_4 , PO_4 , VO_4). The main objectives of this contribution are to (1) reveal the various structures of the YLi_4^+ cations and their stability, (2) calculate the vertical electron affinities (EA_{vert}) of these cations, and explore the correlation between EA_{vert} values and the structural features of YLi_4^+ , (3) discuss whether these species possess superalkali characteristics. We believe that the results in this work will aid in the investigation of polynuclear superalkali clusters with polyvalent central core, and also be useful for the design of new materials in which exceptionally strong reducers are involved.

2. Computational details

The potential energy surfaces of the YLi_4^+ (Y = PO_4 , AsO_4 , VO_4) cations were explored using the randomized algorithms.^{7, 8, 23-27} Firstly, all atoms were placed at a

common point in geometrical space and then were tossed randomly within a sphere with radius between R_{\min} and R_{\max} . We set the $R_{\min} = 1.5 \text{ \AA}$ and $R_{\max} = 6.0 \text{ \AA}$. Such “zero” input structure can avoid biasing the search. Several hundred starting geometries were obtained at the B3LYP/STO-3G level until no new minimum appeared. After that, randomized searches were operated again in the region of one structure found above to do an intensive search for additional minima. The minima at the B3LYP/STO-3G level were then reoptimized at the MP2/6-311+G(3df) level, followed by vibrational frequency calculations. Furthermore, the CCSD(T)/6-311+G(3df) single-point computations on these stable points were carried out. For the vanadium atom, all the calculations were carried out with the LANL2DZ basis set.

The vertical electron affinities (EA_{vert}) of these YLi_4^+ cations were obtained and assigned on the basis of the restricted outer valence Green function (OVGF)²⁸⁻³⁰ method with the 6-311+G(3df) basis set. For some cases where the OVGF approximation may be invalid in view of smaller pole strengths (PSs) than the 0.80-0.85 criterion,³¹ we employed the MP2 method instead and the resulting EA_{vert} values were calculated by subtracting the energies of the corresponding neutrals from those of the YLi_4^+ cations. Natural bond orbital (NBO)³² analyses were performed at the MP2/6-311+G(3df) level. The binding energies per atom (E_b) of YLi_4^+ were obtained at the CCSD(T)/6-311+G(3df) level, where

$$E_b(YLi_4^+) = [3E(Li) + E(Li^+) + E(P / As / V) + 4E(O) - E(YLi_4^+)] / 9$$

All calculations were performed using the *GAUSSIAN 09* program package.³³ Dimensional plots of the molecular structures were generated with the *GaussView* program.³⁴

3. Results and discussion

The optimized geometries of various isomers of YLi_4^+ ($Y = PO_4, AsO_4, VO_4$) are shown in Figures 1-3, respectively. The binding energy values, highest occupied molecular orbital (HOMO)-lowest unoccupied molecular orbital (LUMO) gaps and symmetry of these cations are gathered in Tables 1-3, respectively. In addition, the

zero-point-corrected dissociation energies (E_{dis}) of the fragmentation channel $\text{YLi}_4^+ \rightarrow \text{YLi}_3 + \text{Li}^+$ are obtained at the MP2/6-311+G(3df) level and listed in Tables 1-3, respectively.

For convenience, we name the minimum energy structures of YLi_4^+ **Z1**, **Z2**, **Z3**, **Z4** (**Z** = **P**, **A**, **V** for PO_4Li_4^+ , $\text{AsO}_4\text{Li}_4^+$, VO_4Li_4^+ , respectively)... The total energies of these structures increased in the order **Z1** < **Z2** < **Z3** < **Z4** <..., at the CCSD(T)/6-311+G(3df) level. For comparisons, the electronic and energetic properties of mononuclear superalkali cation NLi_4^+ at the CCSD(T)/MP2/6-311+G(3df) level are also listed in Table 1, the optimized geometries of isolated PO_4^{3-} , AsO_4^{3-} , VO_4^{3-} trianions and the stable Li_3PO_4 , Li_3AsO_4 and Li_3VO_4 compounds obtained at the MP2/6-311+G(3df) level are presented in Figure S1 (Electronic Supplementary Information (ESI)). Their main geometrical parameters are shown in Table S1. The natural bond orbital (NBO) charges of the YLi_4^+ ($\text{Y} = \text{PO}_4$, AsO_4 , VO_4) cations are shown in Tables S2-S4, respectively. Besides, the HOMOs of the representative PO_4Li_4^+ cations are illustrated in Figure S2 to assist in understanding the preference of one isomer over the others.

The vertical electron affinities (EA_{vert}) for the YLi_4^+ ($\text{Y} = \text{AsO}_4$, PO_4 , VO_4) cations, which can reflect the IP of their corresponding neutral parents, are also collected in Tables 1-3, respectively. As expected, these polynuclear cations exhibit very low EA_{vert} values, and can be considered as superalkali or pseudoalkali cations.

In the following subsections, the structural features and stabilities, as well as the EA_{vert} values of the isomers for the YLi_4^+ cations are discussed in detail.

3.1. PO_4Li_4^+ .

Seven structures are identified for the PO_4Li_4^+ cations, which are presented in Figure 1. The most stable isomer of PO_4Li_4^+ , **P1**, exhibits a D_{2d} -symmetrical form where four Li atoms are coplanar. Each Li ligand links two neighbor O atoms and is bound to the central P atom. The configuration of **P1** can be regarded as a Li atom inserted in the lowest energy structure of previously reported superalkali cation SO_4Li_3^+ .²³ The O-Li and Li-P bond lengths of **P1** are 1.913 and 2.417 Å, respectively. The O-P bond length is 1.555 Å, which is slightly shorter compared with that (1.584

Å) of the isolated PO_4^{3-} group. The angles $\angle\text{O1PO2}$ and $\angle\text{O1PO3}$ are 104.5° and 119.9° , respectively. Though the PO_4^{3-} group is clearly distorted from the T_d structure upon the influence of the Li ligands, its structural integrity is maintained in **P1**.

The less favorable structure of PO_4Li_4^+ , **P2**, is higher in energy by 6.70 kcal/mol than **P1**. Isomer **P2** is of C_{3v} symmetry and can be regarded as a Li^+ cation bound to the top O atom of the Li_3PO_4 structure. From Figure 1, Figure S1 and Table S1, the introduction of Li^+ leads to elongated P-O1 bond (from 1.478 to 1.513 Å) and shorter P-O2 bond (from 1.594 to 1.561 Å). Meanwhile, the $\angle\text{O1PO2}$ angle decreased from 115.9° to 113.2° while $\angle\text{O2PO3}$ increased from 102.3° to 105.4° . As a result, the PO_4 group in PO_4Li_4^+ is closer to T_d symmetry than in Li_3PO_4 . Note that the O2-Li bond length of 1.914 Å is much longer than the top O1-Li bond length of 1.693 Å because each bottom Li ligand connects with two O atoms.

The next isomer **P3** is only 2.08 kcal/mol less stable than **P2**. The C_s -symmetrical **P3** can be considered as a Li^+ cation side-on bound to the Li_3PO_4 structure, accompanied by lengthened P-O1 bond (from 1.478 to 1.504 Å) and reduced $\angle\text{O1PO4}$ angle (from 115.9° to 105.9°). Obviously, the distortion of the PO_4^{3-} group in **P3** is a bit larger than that in **P2**.

Among all of the PO_4Li_4^+ structures, the T_d -symmetrical **P4** is the only one without O-Li-O fragments. This might be the reason why it is much higher in energy than the former three isomers. The PO_4^{3-} group maintains its configuration in **P4** except that the latter shows a slightly shorter P-O bond (1.539 Å).

As can be seen from Figure 1, the PO_4 group loses its structural integrity and is cleaved into two fragments by Li atoms in **P5** and latter structures. Isomer **P5** is of C_{3v} -symmetry and 27.42 kcal/mol higher in energy than **P4**. In this structure, three Li atoms link O4 atom with the PO_3 unit. The O1-Li1 bond length of 1.841 Å is quite close to that in the Li_3PO_4 molecule, while the bridged O4-Li1 distance (1.925 Å) is relatively long. In contrast, the O4-Li4 bond is as short as 1.754 Å, which is close to that of LiO^- molecule (1.690 Å at the MP2/6-311+G(3df) level). Hence, **P5** can be viewed as the combination of a LiO^- anion and a $\text{PO}_3\text{Li}_3^{2+}$ ion. This is also supported by the NBO analyses. From Table S2, the NBO charges on the Li4-O4 and PO_3Li_3

units are $-0.709|e|$ and $1.709|e|$, respectively.

The least two favorable structures of PO_4Li_4^+ , namely **P6** and **P7**, are 5.38 and 7.71 kcal/mol less stable than **P5**. They possess C_{2v} and C_s symmetries, respectively. The O2-Li2 and O3-Li3 bond lengths of **P6** are 1.954 Å, which are obviously longer than the other O-Li bond lengths (1.686 ~ 1.747 Å). This indicates that the configuration of **P6** can be viewed as constituted by superalkali cation OLi_3^+ and lithium metaphosphate LiPO_3 . It is clearly seen from Figure S2 that the HOMO of **P6** mainly originates from the OLi_3 moiety. This description is also valid for isomer **P7**, which has a similar geometry to **P6** except that the O1-Li1 bond in **P7** is bent towards O2 atom. Hence, the difference in total energy between **P6** and **P7** is only 2.33 kcal/mol.

From the above results, the stability of the PO_4Li_4^+ isomers is related to the structural integrity of the PO_4 core, and the structures with intact PO_4^{3-} group are more stable than the others. From Figure S2, it is found that the isomer with more even electron cloud distribution usually shows higher stability.

The gap between the highest occupied molecular orbital (HOMO) and the lowest unoccupied molecular orbital (LUMO) is a useful quantity for examining the stability of clusters. It is found that systems with larger HOMO-LUMO energy gaps are less reactive. As listed in Table 1, the HOMO-LUMO gaps of the PO_4Li_4^+ cations are 8.88 ~ 12.87 eV, which are larger than that of mononuclear NLi_4^+ cation (8.20 eV) and comparable to those of 7.58 ~ 10.58 eV for stable superalkali cations OM_3^+ (M = Li, Na, K).³⁵ Meanwhile, the binding energies per atom (E_b) of the PO_4Li_4^+ species are in the 4.925 ~ 5.279 eV range, which are nearly twice those of NLi_4^+ (2.659 eV) and binuclear superalkali cations N_2Li_7^+ (2.530 ~ 2.815 eV).⁸ Besides, the PO_4Li_4^+ cations exhibit positive dissociation energies of 19.61 ~ 89.71 kcal/mol with regard to loss of Li^+ . All of the above energetic properties demonstrate the stability of the polynuclear PO_4Li_4^+ cations.

As can be seen from Table 1, all the PO_4Li_4^+ cations, except **P5**, exhibit fairly low EA_{vert} values of 2.46 ~ 3.36 eV, which are lower than the IP = 3.89 eV of the Cs atom.¹¹ Therefore, these PO_4Li_4^+ species should be classified as superalkali cations.

Herein, isomers **P1**, **P2** and **P4** containing almost intact PO_4 unit have relative lower EA_{vert} values. Note that isomer **P4** shows the lowest EA_{vert} value among all the PO_4Li_4^+ cations, which might be related to its high molecular symmetry (T_d) and even distribution of the excess positive charge. Although isomer **P3** also possesses an integrated PO_4 core, it shows a higher EA_{vert} value because of the uneven distribution of the Li atoms. Among the seven isomers, the largest EA_{vert} value (4.21 eV) is found for isomer **P5**, which should be attributed to the $\text{PO}_3\text{Li}_3^{2+}$ dication contained in this structure.

3.2. $\text{AsO}_4\text{Li}_4^+$

Thirteen conformers of the $\text{AsO}_4\text{Li}_4^+$ cation are illustrated in Figure 2. It can be seen from the figure that the structural integrity of the AsO_4 group maintains inside the first five isomers, namely **A1-A5**.

The most stable isomer of $\text{AsO}_4\text{Li}_4^+$, **A1**, presents similar structural characteristics to **P1**. Likewise, the As-O bond length of **A1** is ca. 0.03 Å shorter than that (1.735 Å) of the isolated AsO_4^{3-} trianion at the same computational level. The angles $\angle\text{O1AsO2}$ and $\angle\text{O1AsO3}$ in isomer **A1** are 101.3° and 127.5°, respectively. Both As-Li and Li-O bond lengths are 0.07 Å longer compared with corresponding those in the stable Li_3AsO_4 molecule.

A Li^+ cation bound to the “top” site of the Li_3AsO_4 configuration (see Figure S1) generates structure **A2**, which is 7.74 kcal/mol less stable than **A1**. Compared with the structure of Li_3AsO_4 , the introduction of Li^+ results in longer As-O1 bond, shorter As-O2 bond, smaller $\angle\text{O1AsO2}$ and larger $\angle\text{O2AsO3}$ angle. In addition, the bottom Li-O bond length of 1.949 Å is much longer than the top Li-O bond length of 1.698 Å.

Isomer **A3** can also be regarded as derived from Li_3AsO_4 , with a Li^+ cation occupying the “bridge” site of the latter. Consequently, the angle $\angle\text{O1AsO4}$ of 103.0° in **A3** is much smaller than that in **A2**. From Figure 2, the major structural difference between isomers **A3** and **A4** is that the Li3 atom attaches to the O2-O3 side in the former while is only linked to the O3 atom in the latter. As a result, the O3-Li3 bond

and $\angle\text{O2AsO3}$ angle in **A4** are 0.2 Å shorter and 11.5° larger than corresponding those in **A3**, respectively. The As-O1 bond in **A4** is almost equal to that in **A3**, and the difference in $\angle\text{O1AsO4}$ between these two structures is only 0.3°. Besides, isomers **A4** and **A3** have the same average As-O bond length of 1.707 Å.

The T_d -symmetrical isomer **A5** is higher in energy by 15.74 kcal/mol than **A4**. The AsO_4^{3-} group totally maintains its geometry in **A5** except that **A5** has a shorter As-O bond length (1.681 Å). Besides, **A5** has the shortest O-Li bond length of 1.657 Å among all the $\text{AsO}_4\text{Li}_4^+$ cations.

It is found from Figure 2 that the structural integrity of the AsO_4 group is broken from isomer **A6** onwards, which gives rise to an obvious increment in relative energy of these structures. It is clear that the AsO_4 core has split into AsO_2 and O_2 units in isomers **A6**, **A8**, **A12** and **A13**. As far as isomers **A7** and **A9** are concerned, they can also be regarded as containing AsO_2 and O_2 components because of long As-O3 bonds (1.996 and 1.933 Å in **A7** and **A9**, respectively). From Table S3, the AsO_2 and O3-O4 units carry $-0.746|e| \sim -1.057|e|$ and $-1.399|e| \sim -1.651|e|$ NBO charges, respectively, in these six structures. Hence, isomers **A6-A9**, **A12**, and **A13** of $\text{AsO}_4\text{Li}_4^+$ can be classified as peroxides with the $(\text{AsO}_2)^-(\text{Li}^+)_4(\text{O}_2)^{2-}$ form. This description is also supported by the fact that the O3-O4 bond lengths (1.513 ~ 1.557 Å) in these species are quite close to that of O-O peroxy bond (1.475 Å).³⁶

From Figure 2, the AsO_2^- and O_2^{2-} fragments are connected by three Li bridge atoms in both **A6** and **A8** isomers. The main structural difference between these two species is the relative position between AsO_2^- and O_2^{2-} units. In **A6**, line O1O2 is parallel to line Li1Li2, and the O3-O4 bond is perpendicular to line Li1Li2. As for **A8**, the case is just reverse. The $\angle\text{O1AsO2}$ angle of 104.5° in **A8** is 4.1° larger than that in **A6**. In isomers **A12** and **A13**, the AsO_2^- and O_2^{2-} units are linked via two Li atoms. According to structural characteristics and NBO analyses, **A13** can be viewed as constituted by lithium meta-arsenite LiAsO_2 and superalkali cation $(\text{O}_2\text{Li}_3)^+$,²⁴ while the characterization of $(\text{LiAsO}_2)\text{Li}^+(\text{Li}_2\text{O}_2)$ is more appropriate for structure **A12**.

That the Li3 and As atoms in **A6** change over generates the configuration of **A7**, and **A7** is only 0.52 kcal/mol less stable than **A6**. Compared with **A6**, isomer **A7** has a

longer As-O1 bond of 1.737 Å and a smaller $\angle O1AsO2$ angle of 94.9°. Isomer **A9** features a Li-tail geometry in which the $\angle O1AsO2$ angle is 4.5° larger than that in **A7**. Meanwhile, **A9** is found to be 2.55 kcal/mol higher in energy than **A7**. Note that **A9** possesses the shortest O3-O4 bond length of 1.513 Å among all the peroxides considered, namely **A6-A9**, **A12** and **A13**.

The AsO_4 group in structures **A10** and **A11** is found to be cleaved into AsO_3 and O fragments, which are bridged by two Li atoms. These two isomers show great structural similarities to **P6** and **P7**, respectively, and likewise can be viewed as constituted by superalkali cation OLi_3^+ and lithium meta-arsenate $LiAsO_3$, which is also supported by NBO analyses. From Table S3 in the Electronic Supplementary Information (ESI), the NBO charges on the OLi_3^+ and $LiAsO_3$ units are 0.915|e| and 0.085|e| respectively for **A10**, and 0.908|e| and 0.092|e| respectively for **A11**.

Clearly, the $AsO_4Li_4^+$ structures with an unbroken AsO_4^{3-} core show higher stability than the other structural isomers. In addition, the $AsO_4Li_4^+$ cation has more isomers compared with $PO_4Li_4^+$ and $VO_4Li_4^+$ species. This is mainly attributed to the existence of meta-arsenite. Accordingly, the AsO_4^{3-} group can also be separated into AsO_2^- and O_2^{2-} fragments other than AsO_3^- and O^{2-} units.

As can be seen from Table 2, the HOMO-LUMO gaps of the $AsO_4Li_4^+$ cations are as large as 8.96 ~ 13.21 eV. Note that the most stable isomer **A1** possesses the highest gap value among all the $AsO_4Li_4^+$ species. The binding energies per atom (E_b) of $AsO_4Li_4^+$ are in the 4.422 ~ 4.810 eV range, which are slightly smaller compared with those of $PO_4Li_4^+$ but much larger than that of mononuclear NLi_4^+ . From Table 2, although all the $AsO_4Li_4^+$ cations exhibit stability with respect to emission of Li^+ , isomer **A13** shows a small dissociation energy (1.82 kcal/mol).

Except for **A6** and **A13**, all the $AsO_4Li_4^+$ cations possess lower EA_{vert} values than the threshold of 3.89 eV¹¹ and can be considered as superalkali cations. Similar to the case for $PO_4Li_4^+$, isomer **A5** has the lowest EA_{vert} value (2.44 eV) because of its high symmetry. Isomer **A2** shows the second lowest EA_{vert} value of 2.89 eV, which profits from its even distribution of Li cations. As one can notice, the distribution of Li cations in isomers **A3** and **A4** are alike. Consequently, their EA_{vert} values are close to

each other, namely 3.36 and 3.23 eV, respectively. Besides, **A4** exhibits a slightly lower EA_{vert} value than **A3** because its Li-tail structure helps to disperse the excess positive charge. For the same reason, the Li3 atom carries more positive charge in **A4** (0.958|e|) than in **A3** (0.912|e|).

3.3. VO_4Li_4^+

Eight structures are obtained for the VO_4Li_4^+ cations. From Figure 3, the first four favorable structures **V1-V4** show great resemblances to those of $\text{AsO}_4\text{Li}_4^+$ cations, respectively. Thus, the structural integrity of the VO_4 core maintains in these isomers. In the D_{2d} -symmetrical **V1**, $\angle\text{O1VO2}$ is smaller by 21.4° than the $\angle\text{O1VO3}$ angle, and the V-O bond length of 1.736 Å is 0.048 Å shorter than that in isolated VO_4^{3-} group.

Similar to structures **P2** and **A2**, **V2** is of C_{3v} symmetry and can be regarded as derived from the stable Li_3VO_4 molecule with an extra apex Li^+ cation. This additional Li^+ cation reduces $\angle\text{O1VO2}$ by 0.7° and enlarges the $\angle\text{O2VO3}$ angle by 0.9° . These changes are smaller compared with corresponding those in isomer **P2** (**A2**).

Both **V3** and **V4** structures possess C_s symmetry and the energy difference between them is 4.71 kcal/mol. Obviously, the distortion of the central VO_4 core in **V3** and **V4** is a bit larger than in **V2**. The V-O1 bond length of 1.680 Å for **V3** is nearly equal to that of **V4** and slightly shorter than that of **V2**. The $\angle\text{O1VO4}$ angles in **V3** and **V4** are 102.4° and 101.8° , respectively, which are much smaller than that of 116.2° for **V2** due to the formation of O1-Li1-O4 linking fragment. Meanwhile, the Li3-O3 bond length of **V4** (1.742 Å) is ca. 0.2 Å shorter than those of **V2** and **V3**.

Isomer **V5** is of C_{2v} symmetry and only 1.09 kcal/mol less stable than **V4**. It can be viewed as the result of cutting off the O4-Li2 and O4-Li4 bonds in structure **V3**. Accordingly, the $\angle\text{O1VO4}$ angle of **V5** is only 2° smaller than that of **V3**. The O2-Li2 bond length in **V5** is 1.726 Å, which is 0.203 Å shorter compared with that of **V3**. From another point of view, this structure can be regarded as a distorted form of **V1**. Similar to **V1**, the four Li atoms and V atom are coplanar in **V5**. According to

the NBO analyses, the VO_4 core carries $-2.590|e| \sim -2.640|e|$ charges in **V1-V5** isomers. Hence, both geometrical and electronic integrities of the VO_4^{3-} group are kept in the first five isomers of the VO_4Li_4^+ cation.

It can be clearly seen from Figure 3 that the VO_4 group has lost its structural integrity and split into two separate units (VO_3 and O) inside isomers **V6**, **V7** and **V8**, which results in sharply increased relative energies of these structures. From Table S4, the VO_3 unit and O4 atom carry $-0.705|e| \sim -1.143|e|$ and $-1.393|e| \sim -1.654|e|$ NBO charges, respectively, indicating that the orthovanadate VO_4^{3-} group has been cleaved into a metavanadate VO_3^- and an O^{2-} anion in these structures. However, isomers **V6**, **V7** and **V8** show different electronic structural characteristics.

Isomer **V6** is of C_{3v} symmetry and higher in energy by 43.51 kcal/mol than **V5**. Herein, the V-O4 distance of 2.015 Å is much longer than the V-O1 bond length of 1.699 Å. The O1-Li1 and O4-Li4 bond lengths (1.789 Å and 1.746 Å, respectively) are obviously shorter than the O4-Li1 distance (2.111 Å). Meanwhile, the length of O4-Li4 bond is near to that of LiO^- anion (1.690 Å at the MP2/6-311+G(3df) level). Thus, this structure can be regarded as a LiO^- anion bound to the $\text{VO}_3\text{Li}_3^{2+}$ unit. Isomer **V7** also possesses C_{3v} symmetry. It looks like an OLi_4^{2+} cation with the addition of a face-capping VO_3^- anion. This description is validated by relatively longer Li1-O2 bond (2.100 Å) than the O4-Li bonds (1.715 ~ 1.846 Å). As for isomer **V8** with C_s symmetry, the VO_3 unit and O4 atom are linked via two Li atoms. Intuitively, the structural difference between **A10** and **V8** is that the former is a planar molecule while the latter is not. The angle $\angle\text{O1VO4}$ is 149.0°. The bridged O2-Li2 and O3-Li3 bond lengths of 1.944 Å are relatively long compared with the other O-Li bond length (1.686 ~ 1.758 Å). So this structure is much like a combination of lithium metavanadate and OLi_3^+ superalkali cation.

From Table 3, all of the VO_4Li_4^+ cations show large HOMO-LUMO gaps ranging from 8.21 to 12.91 eV. Among all of the VO_4Li_4^+ species, the most stable isomer **V1** and the least favorable isomer **V8** exhibit the largest and the smallest gap values, respectively. The E_b values of VO_4Li_4^+ vary in the range of 4.809 ~ 5.215 eV and are slightly larger than those of $\text{AsO}_4\text{Li}_4^+$. Besides, all of the isomers of VO_4Li_4^+

are stable with respect to loss of a Li^+ cation on the basis of the positive dissociation energies.

Except isomer **V6**, all the VO_4Li_4^+ cations exhibit considerably low EA_{vert} values ranging from 2.85 to 3.58 eV and can be viewed as superalkali cations. As expected, the lowest EA_{vert} value is found to belong to isomer **V2**. Isomer **V1** shows the second lowest EA_{vert} value of 2.86 eV because of its high symmetry, which benefits a more even distribution of the excess positive charge. Isomer **V5** has a similar arrangement of Li atoms to that of **V1** and hence shows a comparably low EA_{vert} value. It is known that distributing the Li atoms as far as possible from each other helps to disperse the excess positive charge and therefore reduce the repulsion interaction. On this account, the EA_{vert} value of **V4** is lower than that of **V3**. By the same token, isomer **V8** also possesses a low EA_{vert} value of 3.18 eV though it contains completely cleaved VO_4^{3-} group. As to isomer **V6**, it has a relatively high EA_{vert} value because of the embedded $\text{VO}_3\text{Li}_3^{2+}$ bivalent cation.

4. Conclusions

Our systematic study on polynuclear superalkalis has been extended to the species containing trivalent central core. Theoretical calculations on the YLi_4^+ ($\text{Y} = \text{PO}_4, \text{AsO}_4, \text{VO}_4$) cations reveal that the structures with integrated Y group are more stable than the others. Interestingly, the $\text{AsO}_4\text{Li}_4^+$ cation has more isomers compared with PO_4Li_4^+ and VO_4Li_4^+ since the AsO_4^{3-} group can be separated into meta-arsenite and O_2^{2-} fragments. In comparison with mononuclear superalkali cation NLi_4^+ , the polynuclear YLi_4^+ cations exhibit much large binding energies and comparable HOMO-LUMO gaps. Besides, the global minimum and most low-lying structures of YLi_4^+ show high thermodynamic stability against loss of a Li^+ cation. This also gives evidence of the superatom quality of the investigated cations. And, most importantly, most of the YLi_4^+ species exhibit lower vertical electron affinities than the 3.89 eV threshold and should be classified as superalkali or pseudoalkali cations, especially those with high molecular symmetry.

Electronic supplementary information

The optimized structures and geometrical parameters of isolated PO_4^{3-} , AsO_4^{3-} , VO_4^{3-} , Li_3PO_4 , Li_3AsO_4 and Li_3VO_4 . The NBO charges of the PO_4Li_4^+ , $\text{AsO}_4\text{Li}_4^+$, VO_4Li_4^+ cations. The highest occupied molecular orbitals of the PO_4Li_4^+ cations.

Acknowledgement

This work was supported by the National Natural Science Foundation of China (Grant Nos. 21173095, 21173098, 21303066) and the National Basic Research Program of China (2013CB834801).

Notes and references

1. S. N. Khanna and P. Jena, *Phys. Rev. Lett.*, 1992, **69**, 1664.
2. S. N. Khanna and P. Jena, *Phys. Rev. B*, 1995, **51**, 13705.
3. G. L. Gutsev and A. I. Boldyrev, *Chem. Phys. Lett.*, 1982, **92**, 6.
4. E. Rehm, A. I. Boldyrev and P. v. R. Schleyer, *Inorg. Chem.*, 1992, **31**, 4834.
5. D. L. Chen, W. Q. Tian, W. C. Lu and C. C. Sun, *J. Chem. Phys.*, 2006, **124**, 154313.
6. Y. Li, D. Wu, Z. R. Li and C. C. Sun, *J. Comput. Chem.*, 2007, **28**, 1677.
7. J. Tong, Y. Li, D. Wu, Z. R. Li and X. R. Huang, *J. Chem. Phys.*, 2009, **131**, 164307.
8. J. Tong, Y. Li, D. Wu, Z. R. Li and X. R. Huang, *J. Phys. Chem. A*, 2011, **115**, 2041.
9. S. Zein and J. V. Ortiz, *J Chem Phys*, 2011, **135**, 164307.
10. S. Zein and J. V. Ortiz, *J Chem Phys*, 2012, **136**, 224305.
11. S. G. Lias, J. E. Bartmess, J. F. Liebman, J. L. Homes, R. D. Levin and W. G. Mallard, *J. Phys. Chem. Ref. Data, Suppl.*, 1988, **17**, 1285.
12. E. Zintl and M. Z. Morawietz, *Z. Anorg. Allg. Chem.*, 1938, **236**, 372.
13. V. M. Jansen, *Angew. Chem.*, 1976, **88**, 411.
14. V. M. Jansen, *Z. Anorg. Allg. Chem.*, 1977, **435**, 13.
15. V. M. Jansen, *Z. Naturforsch.*, 1982, **34a**, 1457.
16. A. C. Reber, S. N. Khanna and A. W. J. Castleman, *J. Am. Chem. Soc.*, 2007, **129**, 10189.
17. F. F. Wang, Z. R. Li, D. Wu, X. Y. Sun, W. Chen, Y. Li and C. C. Sun, *ChemPhysChem*, 2006, **7**, 1136.
18. Y. Li, D. Wu and Z. R. Li, *Inorg. Chem.*, 2008, **47**, 9773.
19. I. Anusiewicz, *Aust. J. Chem.*, 2010, **63**, 1573.
20. H. Yang, Y. Li, D. Wu and Z. R. Li, *Int. J. Quantum. Chem.*, 2012, **112**, 770.
21. S. Giri, S. Behera and P. Jena, *J. Phys. Chem. A*, 2014, **118**, 638.
22. I. Anusiewicz, *J. Theor. Comput. Chem.*, 2011, **10**, 191.
23. J. Tong, Y. Li, D. Wu and Z. J. Wu, *Inorg. Chem.*, 2012, **51**, 6081.
24. J. Tong, Z. J. Wu, Y. Li and D. Wu, *Dalton. Trans.*, 2013, **42**, 577.

25. M. Saunders, *J. Comput. Chem.*, 2004, **25**, 621.
26. P. P. Bera, K. W. Sattelmeyer, M. Saunders, H. F. Schaefer and P. v. R. Schleyer, *J. Phys. Chem. A*, 2006, **110**, 4287.
27. D. Roy, C. Corminboeuf, C. S. Wannere, R. B. King and P. v. R. Schleyer, *Inorg. Chem.*, 2006, **45**, 8902.
28. L. S. Cederbaum, *J. Phys. B: At. Mol. Phys.*, 1975, **8**, 290.
29. J. V. Ortiz, *J. Chem. Phys.*, 1988, **89**, 6348.
30. V. G. Zakrzewski, W. v. Niessen, A. I. Boldyrev and P. v. R. Schleyer, *Chem. Phys.*, 1993, **174**, 167.
31. V. G. Zakrzewski, O. Dolgounitcheva and J. V. Ortiz, *J. Chem. Phys.*, 1996, **105**, 5872.
32. A. E. Reed, R. B. Weinstock and F. Weinhold, *J. Chem. Phys.*, 1985, **83**, 735.
33. M. J. Frisch, G. W. Trucks, H. B. Schlegel, G. E. Scuseria, M. A. Robb, J. R. Cheeseman, V. B. G. Scalmani, B. Mennucci, G. A. Petersson, H. Nakatsuji, M. Caricato, X. Li, H. P. Hratchian, A. F. Izmaylov, J. Bloino, G. Zheng, J. L. Sonnenberg, M. Hada, M. Ehara, K. Toyota, R. Fukuda, J. Hasegawa, M. Ishida, T. Nakajima, Y. Honda, O. Kitao, H. Nakai, T. Vreven, J. A. Montgomery, J. E. P. Jr., F. Ogliaro, M. Bearpark and E. B. J. J. Heyd, K. N. Kudin, V. N. Staroverov, R. Kobayashi, J. Normand, K. Raghavachari, A. Rendell, J. C. Burant, S. S. Iyengar, J. Tomasi, M. Cossi, N. Rega, J. M. Millam, M. Klene, J. E. Knox, J. B. Cross, V. Bakken, C. Adamo, J. Jaramillo, R. Gomperts, R. E. Stratmann, O. Yazyev, A. J. Austin, R. Cammi, C. Pomelli, J. W. Ochterski, R. L. Martin, K. Morokuma, V. G. Zakrzewski, G. A. Voth, P. Salvador, J. J. Dannenberg, S. Dapprich, A. D. Daniels, O. Farkas, J. B. Foresman, J. V. Ortiz, J. Cioslowski, and D. J. Fox, Gaussian, Inc, Wallingford, CT, *GAUSSIAN 09*, revision A01 ed., 2009.
34. R. H. Dennington, K. Todd, J. Millam, K. Eppinnett, W. L. Hovell and R. Gilliland, in *GaussView*, Semichem Inc, Shawnee Mission, KS, version 3.09 ed., 2003.
35. J. Tong, Y. Li, D. Wu and Z. J. Wu, *Chem. Phys. Lett.*, 2013, **575**, 27.
36. *CRC Handbook of Chemistry and Physics*, CRC press, Boca Raton, Florida, Lide, David R ed., 2008.

Table 1. Symmetry Point Group, the Lowest Vibrational Frequencies (ν_1 , in cm^{-1}), Relative Energies (E_{rel} , in kcal/mol), HOMO–LUMO Gaps (in eV), Binding Energies per Atom, (E_{b} , in eV), Dissociation Energy (E_{dis} , in kcal/mol) and Vertical Electron Affinities (EA_{vert} , in eV) of the PO_4Li_4^+ and NLi_4^+ Cations.

| isomer | symmetry | ν_1 | E_{rel} | Gap | E_{b} | E_{dis} | EA_{vert} |
|------------------------------------|----------|---------|------------------|-------|----------------|------------------|--------------------|
| P1 | D_{2d} | 136 | 0.00 | 12.87 | 5.279 | 89.71 | 2.96 |
| P2 | C_{3v} | 84 | 6.70 | 12.15 | 5.246 | 83.44 | 2.82 |
| P3 | C_s | 157 | 8.78 | 12.14 | 5.236 | 81.37 | 3.24 |
| P4 | T_d | 23 | 38.29 | 10.53 | 5.094 | 53.15 | 2.46 |
| P5 | C_{3v} | 86 | 65.71 | 11.87 | 4.962 | 26.29 | 4.21 |
| P6 | C_{2v} | 36 | 71.09 | 8.88 | 4.936 | 21.77 | 3.28 |
| P7 | C_s | 41 | 73.42 | 9.44 | 4.925 | 19.61 | 3.36 |
| NLi₄⁺ | T_d | 218 | - | 8.20 | 2.659 | 90.05 | 3.48 |

Table 2. Symmetry Point Group, the Lowest Vibrational Frequencies (ν_1 , in cm^{-1}), Relative Energies (E_{rel} , in kcal/mol), HOMO–LUMO Gaps (in eV), Binding Energies per Atom, (E_{b} , in eV), Dissociation Energy (E_{dis} , in kcal/mol) and Vertical Electron Affinities (EA_{vert} , in eV) of the $\text{AsO}_4\text{Li}_4^+$ Cations.

| isomer | symmetry | ν_1 | E_{rel} | Gap | E_{b} | E_{dis} | EA_{vert} |
|------------|----------|---------|------------------|-------|----------------|------------------|--------------------|
| A1 | D_{2d} | 148 | 0.00 | 13.21 | 4.810 | 86.58 | 3.02 |
| A2 | C_{3v} | 74 | 7.74 | 12.51 | 4.772 | 79.00 | 2.89 |
| A3 | C_s | 167 | 10.70 | 12.55 | 4.758 | 76.19 | 3.36 |
| A4 | C_s | 31 | 16.84 | 11.94 | 4.729 | 70.22 | 3.23 |
| A5 | T_d | 38 | 32.58 | 11.00 | 4.653 | 55.12 | 2.44 |
| A6 | C_s | 89 | 64.31 | 11.93 | 4.500 | 16.79 | 3.90 |
| A7 | C_1 | 71 | 64.83 | 10.35 | 4.497 | 16.23 | 3.30 |
| A8 | C_s | 25 | 66.91 | 11.92 | 4.487 | 14.48 | 3.69 |
| A9 | C_1 | 121 | 67.38 | 10.19 | 4.485 | 12.84 | 3.62 |
| A10 | C_{2v} | 30 | 67.53 | 8.96 | 4.484 | 21.85 | 3.30 |
| A11 | C_s | 34 | 69.46 | 9.44 | 4.475 | 20.07 | 3.68 |
| A12 | C_s | 39 | 74.27 | 11.06 | 4.452 | 7.92 | 3.36 |
| A13 | C_s | 35 | 80.54 | 10.86 | 4.422 | 1.82 | 4.01 |

Table 3. Symmetry Point Group, the Lowest Vibrational Frequencies (ν_1 , in cm^{-1}), Relative Energies (E_{rel} , in kcal/mol), HOMO–LUMO Gaps (in eV), Binding Energies per Atom, (E_{b} , in eV), Dissociation Energy (E_{dis} , in kcal/mol) and Vertical Electron Affinities (EA_{vert} , in eV) of the VO_4Li_4^+ Cations.

| isomer | symmetry | ν_1 | E_{rel} | Gap | E_{b} | E_{dis} | EA_{vert} |
|-----------|----------|---------|------------------|-------|----------------|------------------|--------------------|
| V1 | D_{2d} | 144 | 0.00 | 12.91 | 5.215 | 81.08 | 2.86 |
| V2 | C_{3v} | 79 | 7.11 | 12.12 | 5.181 | 72.73 | 2.85 |
| V3 | C_s | 177 | 10.39 | 12.19 | 5.165 | 73.00 | 3.30 |
| V4 | C_s | 64 | 15.10 | 11.77 | 5.143 | 69.14 | 3.03 |
| V5 | C_{2v} | 29 | 16.19 | 11.56 | 5.137 | 66.22 | 2.90 |
| V6 | C_{3v} | 92 | 59.70 | 10.07 | 4.928 | 29.79 | 4.67 |
| V7 | C_{3v} | 146 | 62.61 | 10.13 | 4.914 | 31.40 | 3.58 ^a |
| V8 | C_s | 29 | 84.39 | 8.21 | 4.809 | 12.95 | 3.18 ^a |

^a Calculated at the MP2/6-311+G(3df) level.

Figure 1. Seven equilibrium structures of polynuclear cation PO_4Li_4^+ . Color legend: P, orange; O, red; Li, purple.

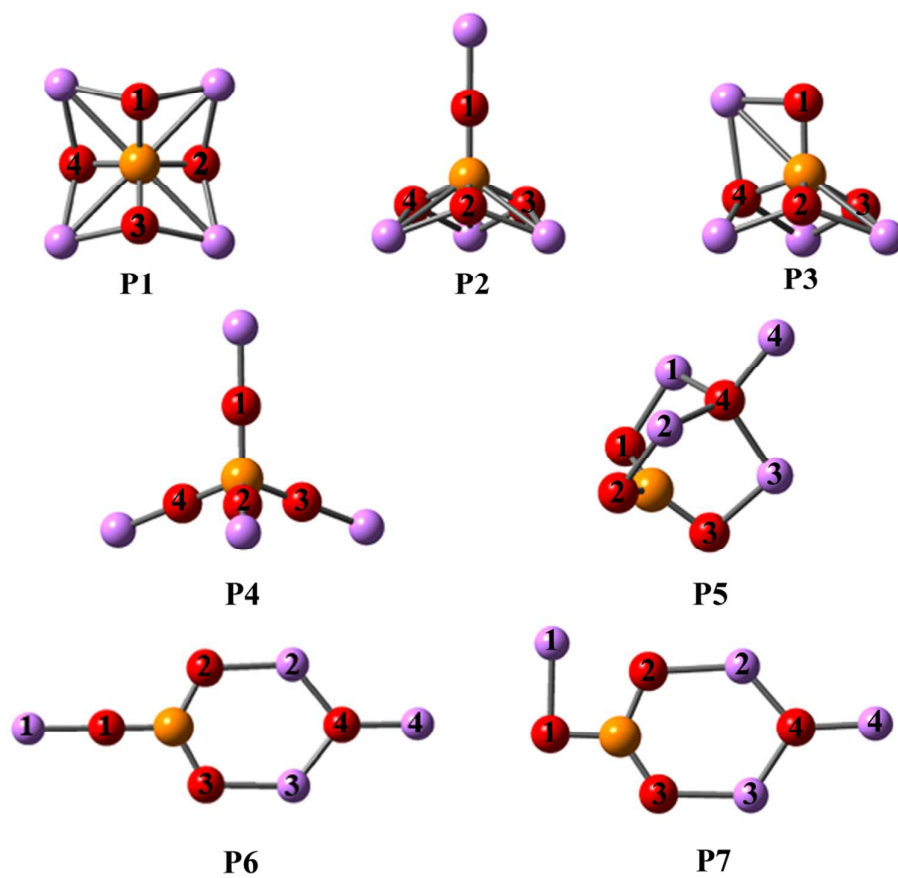


Figure 2. Thirteen equilibrium structures of polynuclear cation $\text{AsO}_4\text{Li}_4^+$. Color legend: As, mazarine; O, red; Li, purple.

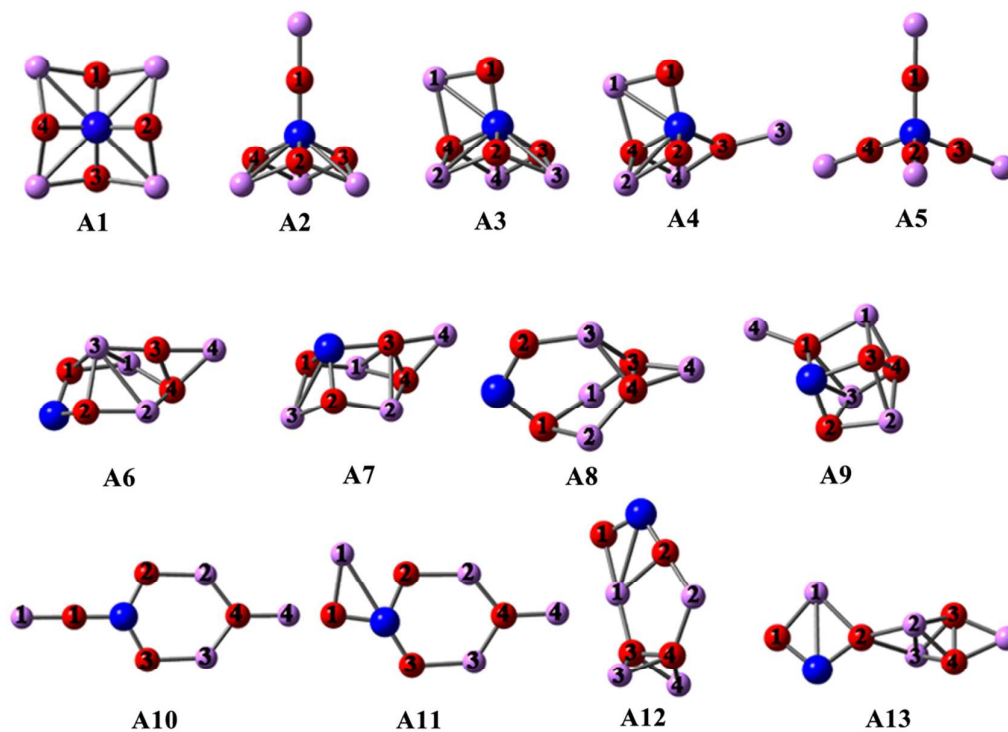


Figure 3. Eight equilibrium structures of polynuclear cation VO_4Li_4^+ . Color legend: V, grey; O, red; Li, purple.

